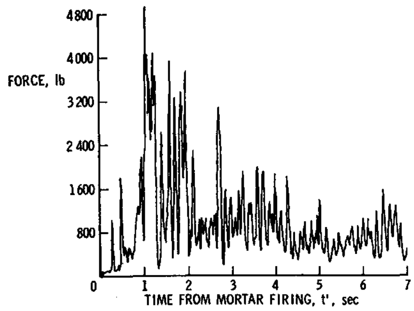

Fig. 6 Time history of force measured by the tensiometer.

for a calm day employing excursions measured directly from high-speed motion-picture film are compared in Table 3, and Fig. 5 shows the transient load curves for the same three tests. In the second drop-test series (Fig. 4), an opening shock load of 6230–6300 lb was followed by a sustained load of 5550 lb. All elements of the damper were fully elongated without failure.

Two sets of a flight-type energy absorber hardware (Fig. 2) were then taken to El Centro, Calif. for low-altitude drop tests. The damper bundle of each flight article comprised 53 layers of PVC film with a total thickness of 0.45 in. (1.14 cm). Two break straps of dacron (not shown in Fig. 2) restrained the PVC from opening until the onset of the initial maximum canopy inflation. The primary objective of demonstrating extraction of the absorber from its small-clearance fit in the payload canister without damage was accomplished in both tests, but these low-altitude drops from helicopters were nonrepeatable with regard to opening shock level, such that attenuation capability relative to the undamped system could not be determined. Examination of the recovered absorbers indicated that interlayer friction caused fusing of the PVC layers in the damper bundle during operation. Therefore, one change made for supersonic flight test items was the use of talcum powder sprinkled between the PVC layers.

In the Mach 3.3 flight at the White Sands Missile Range, New Mexico, all elements of the energy absorber performed their designed functions. The initial load peak at 1.03 sec after mortar firing (Fig. 6) produced a 21.1-g deceleration and was associated with the breaking of the aforementioned dacron break straps. Subsequent loads did not exceed the $\sim$15-g deceleration load for which the absorber had been designed. Other occurrences during the mission, however, preclude complete assessment of the absorber effectiveness. Details of the canopy damage which is believed to have been caused by aerodynamic heating and which could have also have a load-alleviating effect are given in Ref. 3. Response characteristics for a Mach 2.7 flight without the attenuator are compared with those for the Mach 3.3 flight with the attenuator in Fig. 7. Although higher loads would have been anticipated for the latter flight based on extrapolation of earlier undamped flight data, it can be seen that the load levels were considerably reduced.

Concluding Remarks

It is felt that the absorber appreciably reduced the severity of the payload response to parachute opening shock loads, and that better stroke and absorption characteristics could be obtained if the design were not limited by volumetric constraints. It is recommended that consideration be given to the development of lightweight, long-stroke energy absorption devices.

Table 3 Load amplitude data—drop series I

Test no.	Configuration	Load at first rebound, lb	Drop distance, ft	Rebound height, ft
5, 7	Undamped	5000, 4950	55	22.5
6	Damped	2720	55	10.6

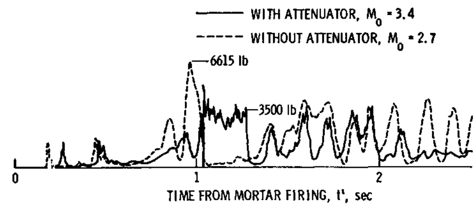

Fig. 7 Flight tensiometer records.

References

[1] Preisser, J. S. and Eckstrom, C. V., "Flight Test of a 40-Foot-Nominal-Diameter Disk-Gap-Band Parachute Deployed at a Mach Number of 1.91 and a Dynamic Pressure of 11.6 Pounds Per Square Foot," TM X-1575, 1968, NASA.

[2] Eckstrom, C. V. and Preisser, J. S., "Flight Test of a 40-Foot-Nominal-Diameter Disk-Gap-Band Parachute Deployed at a Mach Number of 2.72 and a Dynamic Pressure of 9.7 Pounds Per Square Foot," TM X-1623, 1968, NASA.

[3] Eckstrom, C. V., "Flight Test of a 40-Foot-Nominal-Diameter Disk-Gap-Band Parachute Deployed at a Mach Number of 3.31 and a Dynamic Pressure of 10.6 Pounds Per Square Foot," TM X-1924, 1970, NASA.

[4] Gray, J. H., "Attenuation of Deployment and Opening Forces of Certain Aerodynamic Decelerators," *Proceedings—Symposium on Parachute Technology and Evaluation,* Vol. II, edited by Earl C. Myers, FTC-TDR-64-12, U.S. Air Force, 1964, pp. 502–508.

[5] Preisser, J. S. and Eckstrom, C. V., "Flight Test of a 30-Foot-Nominal-Diameter Cross Parachute Deployed at a Mach Number of 1.57 and a Dynamic Pressure of 9.7 Pounds Per Square Foot," TM X-1542, 1968, NASA.

A Shielded Fine-Wire Probe for Rapid Measurement of Total Temperature in High-Speed Flows

LEONARD M. WEINSTEIN*
NASA Langley Research Center, Hampton, Va.

Nomenclature

A = parameter defined as $(k_0/k)^{1/2}Nu^{1/2}L/D$
d = probe height, in.
K_d = Knudsen number, $(= 1.26\gamma^{1/2}M_\infty/Re_{\infty,d})$
k = thermal conductivity of wire material
k_0 = thermal conductivity of gas evaluated at the gas total temperature
M = Mach number
p = pressure
$Re_{\infty,d}$ = Reynolds number $\rho_\infty u_\infty d/\mu_\infty$
Re_i, Re_0 = $\rho_i u_i d/\mu_{t,\infty}$ and $\rho_\infty u_\infty d/\mu_{t\infty}$, respectively
L/D = length diameter ratio of sensing wire
Nu = Nusselt number
R_w = resistance of wire, ohms
T = temperature, °R
u = gas velocity, fps
γ = ratio of specific heats
ξ = $(T_t - T_w)/(T_t - T_s)$
Φ = $\xi/(1-\xi) = (T_t - T_w)/(T_w - T_s)$
ρ,μ = density and viscosity, respectively

Received November 2, 1970; revision received December 21, 1970.
* Aerospace Engineer, Aero-Physics Division.

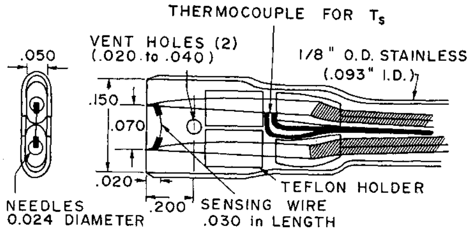

Fig. 1 Probe geometry.

Subscripts

aw = adiabatic wall
c = calibrated
i = internal shield stream value (near the probe wire)
max = maximum
r = test value
s = probe support needles
t = total
w = wire
∞ = local freestream value
1,2 = probe identification

Introduction

THE most common method of measuring total temperature in high-speed flow utilizes a shielded thermocouple.[1,2] The velocity of the external flow decreases inside the shield, but remains sufficiently high so that the convective heat imput is large enough to minimize the effects of conduction and radiation.[3,4] Other useful methods include unshielded resistance wires[5] and hot wires.[6,7] The type of probe used depends on such factors as response time, accuracy, calibration requirements, ability to withstand expected environment, spatial resolution, cost and availability, and ease of use. For low-density flows, however, typical probes do not satisfy one or more of these factors and often given questionable results. Strong dependence of probe recovery factor on M, Re, K_d, conduction down the sensing element supports, and uncertainty in the values of local flow parameters often make calibration procedures doubtful.

This Note describes a shielded, thin-wire, total temperature probe (reported in Ref. 8 in an earlier version), which was developed to satisfy the test requirements for a hypersonic helium facility having a 4- to 6-sec run time. The probe can survey across a 1-in. hypersonic boundary layer in ~2 sec, generally gives better than $\frac{1}{4}\%$ absolute accuracy in the reduced data, is useful for $M_\infty > 1$, $Re_0 > 10$ (based on a 0.050-in. probe height), $K_d \leq 0.3$ and, in the present form, for $T_t < 700° R$ (up to the melting point of the solder used in construction). This probe is compared with more conventional types.

Probe Construction

This probe is basically a resistance thermometer positioned in the relatively low-speed flow inside a vented shield. The wire used is 0.00014-in.-diam tungsten with a 0.030-in. sensing length. In addition, the wire is copper coated to a diameter of 0.001 in. on each side of the sensing length for a total length (both ends and the sensing length) of 0.070 in. The copper-coated ends were tinned and soft-soldered to support needles. The needles, supported in teflon sleeves, were then pressed flush with the shield tip so that the sensing wire was 0.020 in. inside the tip (Fig. 1). The shield minimum height of 0.050 in. is typical of sizes used.

The thermal response time is 1–10 msec for most test conditions. For the early version of this probe,[8] a recovery factor of unity was assumed, resulting in a T_t profile which was lower than expected. Later calibrations at low Re's corresponding to locations deep in the boundary layer showed the need to include conduction effects. A data reduction method that follows, using both indicated wire temperature and probe needle temperature, is adequate to obtain high accuracy. (In Ref. 5 a more complex scheme using an unshielded thin wire and monitored end support is described.) In comparison, thermocouple probes have small length/diameter ratios, and thus conduction errors can be large; also, the larger wire size and generally even larger junction result in poor time response. Unshielded thin-wire probes have good time response, better spatial resolution, and less interference than the shielded one described here. However, K_d must be based on wire rather than probe height, resulting in transitional and free molecular flow over a large part of a typical test range. In this case, calibration and data interpretation become difficult, since the probe reading is now strongly dependent on K_d,M, accommodation coefficient, and flow direction, parameters that are not important for the shielded wire (except for a slight Mach number effect at the lower M's; see next section).

Hot wires can also be used for T_t measurements, but they generally have to be operated at several overheats and extrapolated to zero overheat, a time-consuming procedure (pulse heating can also be used,[6] but the accuracy is not as good as it is for the probe described here), and the same problems as for the unshielded thin wire are encountered, as well as large end conduction at nonzero overheats.

Theoretical Considerations

When shielded probes are used in $M_\infty > 1$ flow, the post-shock conditions and shield internal geometry generally govern the flow through the probe. An examination of the appropriate gas flow equations,[9] when $\gamma = \frac{5}{3}$ is used for helium, allows a direct relation to be found between $\rho_i u_i$ and $\rho_\infty u_\infty$ with M_i and M_∞ as the only variables. Since M_i is only a function of probe geometry (if the internal viscous effects are small and the vent hole sonic, both of which are generally true), for a given probe,

$$Re_i \propto Re_0 f(M_\infty) \simeq Re_0(1 - 0.314/M_\infty) \quad (1)$$

where $f(M_\infty)$ is approximated by $(1 - 0.314/M_\infty)$ within 1% of exact values for $M_\infty > 1$.

The effect of probe wire conduction[10] can be written as:

$$\xi = (T_t - T_w)/(T_t - T_s) = [\tanh(A)]/A \quad (2)$$

where $A \equiv (k_0/k)^{1/2} Nu^{1/2} L/D$; $Nu = a + bRe^n$; and a,b, and n are constants.

For a given probe, a fixed M_i results in a unique Nu vs Re_i relationship, and then from Eq. (1), Nu will be directly related to $Re_0(1 - 0.314/M_\infty)$, with a different relation for each probe. Except for other probe constants, such as L/D,ξ is a function only of Nu and k_0/k. The hyperbolic tangent function can be expanded in a series of the form:

$$\tanh A = (1 - \mathrm{sech}^2 A)^{1/2} = [1 - (1 + A^2 + \tfrac{1}{3}A^4 \ldots)^{-1}]^{1/2} \quad (3)$$

Truncating the series to two terms (which gives fair results over all A), Eq. (2) becomes

$$\xi = (1 + A^2)^{-1/2} \quad (4)$$

By calibrating a probe in known flow, one obtains a relation between ξ and $[Re_0(1 - 0.314/M_\infty)]$, and calibration could be extended to flows at greatly different temperatures by taking the variation in (k_0/k) into consideration. This last requires a knowledge of the variation of k and k_0 with T. For helium and tungsten, from Ref. 11, $(k_0/k)_T = T/0.57 \times 10^6$, when T is in °R, for the range $300 < T < 1000$°R. For this case we used Eq. (4) for a probe at different T (holding everything else the same). If we calibrate a probe at conditions with c subscript, and run the test at condi-

Table 1 Operating parameters

Nozzle	M_∞	T_t(°R)	p_t(psia)	Re_0	K_d
3-in.	17–22	540	200–2500	250–1500	0.014–0.14
Low-density	3–5	540	0.2–7	20–1000	0.008–0.3

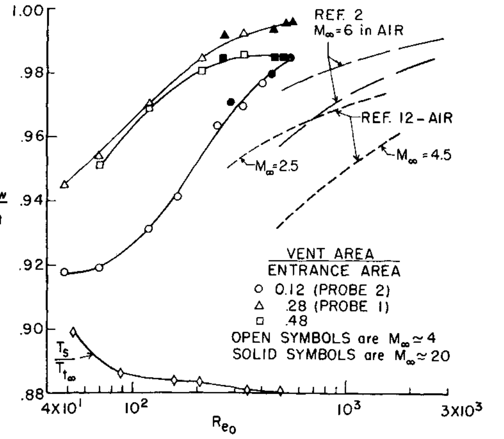

Fig. 2 Calibration curves for various area ratios in helium, and comparison with results from shielded thermocouple probes.

tions with r subscript we have:

$$\xi_r = \{(T_r/T_c)[(T_c/T_r - 1) + \xi_c^{-2}]\}^{-1/2} \quad (5)$$

For other materials, or a temperature beyond the range covered, a correction must be based on the appropriate conductivity ratio. If the T_t used in calibration is close to the test value, the temperature correction can probably be neglected. Solving the ξ parameter for T_t,

$$T_t = T_w + (T_w - T_s)\phi \quad (6)$$

where $\phi = \xi/(1 - \xi)$.

With Re_0 and M_∞ known and T_w and T_s both measured, T_t can be obtained directly from the calibration. If Re_0 and M_∞ are not known, both T_t and the parameter $Re_0(1 - 0.314/M_\infty)$ can be obtained from two of the new probes (which may be housed in the same body) in the following manner. For two probes at the same T_t, we obtain:

$$T_{w1} + \phi_1(T_{w1} - T_{s1}) = T_{w2} + \phi_2(T_{w2} - T_{s2}) \quad (7)$$

or

$$\phi_1 = \frac{T_{w2} - T_{w1}}{T_{w1} - T_{s1}} + \phi_2 \frac{T_{w2} - T_{s2}}{T_{w1} - T_{s1}} \quad (8)$$

From the calibration in the form of ϕ vs $Re_0(1 - 0.314/M_\infty)$, ϕ_1 can be found as a function of ϕ_2 and the resultant calibration line will intersect the line in Eq. (8) for given data. The value of either ϕ_1 or ϕ_2 can be used in Eq. (6) along with data to obtain T_t. In addition, $Re_0(1 - 0.314/M_\infty)$ can be found from the calibration, and if even an approximate value of M_∞ is used, Re_0 can be fairly accurately obtained.

Calibration and Test of Theory

For calibration and preliminary testing of the new probe, a 3-in. exit-diam conical nozzle and a low-density calibration nozzle were used. The operating parameters (using d = 0.050-in.) are given in Table 1.

Calibrations for three probes with different vent-to-entrance area ratios are shown in Fig. 2 in the form of T_w/T_t vs Re_0 to allow comparison with other type probes. At the area ratio near the "optimum" from Ref. 4 (area ratio of 0.28), T_w/T_t is about 0.995 at the highest Re_0. Both larger and smaller area ratios had lower T_w/T_t but the value of T_w/T_t for the smaller vent probe is still increasing rapidly with increasing Re_0 and might approach 1 for very large Re_0. The value of T_w/T_t for the larger vent probe seems to be leveling off at $T_w/T_t = 0.984$, which is due to high M_i (probably near M_i = 0.2 from the area ratio). The support needle temperatures (which were the same for all probes) are shown as T_s/T_t for various Re_0 in the low-density facility. If $Re_0(1 - 0.314/M_\infty)$ were used here instead of just Re_0, the open symbols would shift to the left 5–10% and better agree with the trend of the solid symbols as would be expected.

Fig. 3 Final calibration curves in helium.

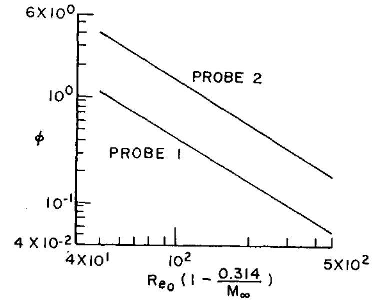

For comparison, data for thermocouple type shielded probes in air[2,12] are included in the figure. Curves from Ref. 2 show the variation that different probes in the same flow can experience—strongly pointing to the need for individual calibration. The curves from Ref. 12 are for M_∞ = 2.5 and 4.5, but, since the flow at these two M_∞'s cool the probe body by different amounts, taking the different T_s/T_t (which were not measured) into account would probably account for some of the apparent M_∞ effect.

Figure 3 shows ϕ vs $Re_0(1 - 0.314/M_\infty)$ for the two smaller-vent-sized new probes in log-log form. Both curves exhibit a power law behavior with virtually equal exponents. From this plot, if ϕ_1 is now plotted against ϕ_2 on a linear plot, a straight line that goes through the origin is obtained by fairing the data (Fig. 4). Equation (8) gives a different straight line on this plot for measured values of T_w and T_s and, if the measured values are used here that were obtained during check runs for values of $Re_0(1 - 0.314/M_\infty)$ = 50 and 200, then the two dashed lines are generated. Where the calibration ϕ_1 vs ϕ_2 and the data used in Eq. (8) cross, values of ϕ_1 and ϕ_2 are determined, either of which can be used in Eq. 6 along with the corresponding T_w and T_s to obtain T_t. In addition, if M_∞ is found even approximately, then Re_0 can be determined from the calibration (Fig. 3).

In conclusion, the total temperature probe described herein satisfies the test requirements for an unheated hypersonic helium facility. It has good time response ($\leq$10 msec), and can give high absolute accuracy when used in connection with probes which help to determine the Re_0 and M_∞ in the flow. When Re_0 and Me_∞ are not known, two of the probes, which can be mounted in a common body or set side by side, are sufficient to determine T_t and also give Re_0 if M_∞ can be approximated. These probes are reasonably easy to make and calibrate, and the test results are valid over wide ranges of test conditions. Some of the calibration and interpretation features described can also be used with many thermo-

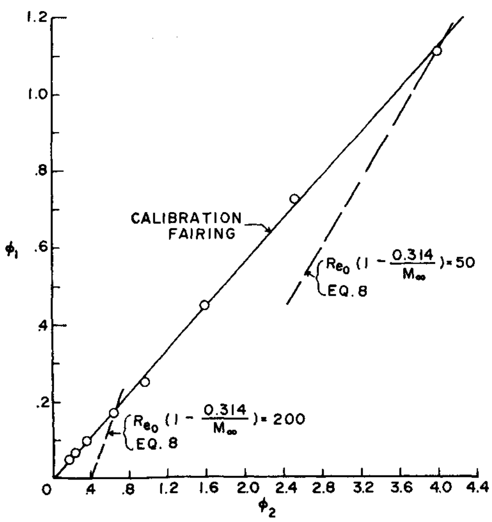

Fig. 4 Two probe determination in helium of T_t from calibration and Eq. (8) in text.

couple probes, if speed of response is not of prime importance. If, for instance, the governing conduction temperature is monitored, then errors due to nonuniform flow around the probe body can be reduced by a data reduction scheme accounting for conduction effects.

References

[1] Hill, F. K., "Turbulent Boundary Layer Measurements at Mach Numbers from 8 to 10," *The Physics of Fluids*, Vol. 2, No. 6, Nov.–Dec. 1959.

[2] Jones, R. A. and Feller, W. V., "Preliminary Surveys of the Wall Boundary Layer in a Mach 6 Axisymmetric Tunnel," TN D-5620, Feb. 1970, NASA.

[3] Goldstein, D. L., and Scherrer, R., "Design and Calibration of a Total Temperature Probe for Use at Supersonic Speeds," TN 1885, 1949, NACA.

[4] Winkler, E. M., "Design and Calibration of Stagnation Temperature Probes for use at High Supersonic Speeds and Elevated Temperatures," *Journal of Applied Physics*, Vol. 25, No. 2, Feb. 1954, pp. 231–232.

[5] Yanta, W. J., "A Hot-Wire Stagnation Temperature Probe," TR 68-60, June 1968, Naval Ordnance Lab, White Oaks, Md.

[6] Softley, E. J., "Use of a Pulse Heated Fine Wire Probe for the Measurement of Total Temperatures in Shock Driven Facilities," TIS R 68SD2, Feb. 1968, General Electric Co.

[7] Wagner, R. D., Jr. et al., "Influence of Measured Freestream Disturbances on Hypersonic Boundary-Layer Transition," *AIAA Journal*, Vol. 8, No. 9, Sept. 1970, pp. 1664–1670.

[8] Fischer, M. C., Maddalon, D. V., and Weinstein, L. M., "Boundary Layer Surveys on a Nozzle Wall at $M_\infty = 20$ Including Hot Wire Fluctuation Measurements," AIAA Paper 70-746, Los Angeles, Calif., 1970.

[9] Ames Research Center Staff, "Equations, Tables, and Charts for Compressible Flow," Rept. 1135, 1953, NACA.

[10] Maye, J. P., "Error Due to Thermal Conduction Between the Sensing Wire and Its Supports When Measuring Temperatures with a Wire Anemometer Used as a Resistance Thermometer," Information 9, Feb. 1970, DISA, Elektronik A/S, Herlev, Denmark.

[11] Kreith, F., *Principles of Heat Transfer*, 2nd ed., International Textbook, Scranton, Pa., 1965.

[12] Adcock, J. B., and Peterson, J. B., Jr., "Experimental Investigation of a Turbulent Boundary Layer at Mach 6, High Reynolds Numbers, and Zero Heat Transfer," TN D-2907, July 1965, NASA.

Unmanned Lunar Logistics Vehicle May Support the Astronauts

FRANK J. HENDEL*
California State Polytechnic College, San Luis Obispo, Calif.

FOR a program of extended lunar exploration under consideration is the addition of an unmanned lunar logistics vehicle (LLV) which will deliver a 2500-lb payload anywhere on the moon's visible face. The spacecraft will be launched by the Titan IIID/Centaur, using at Cape Kennedy the same launch facility as the project Viking.[1]

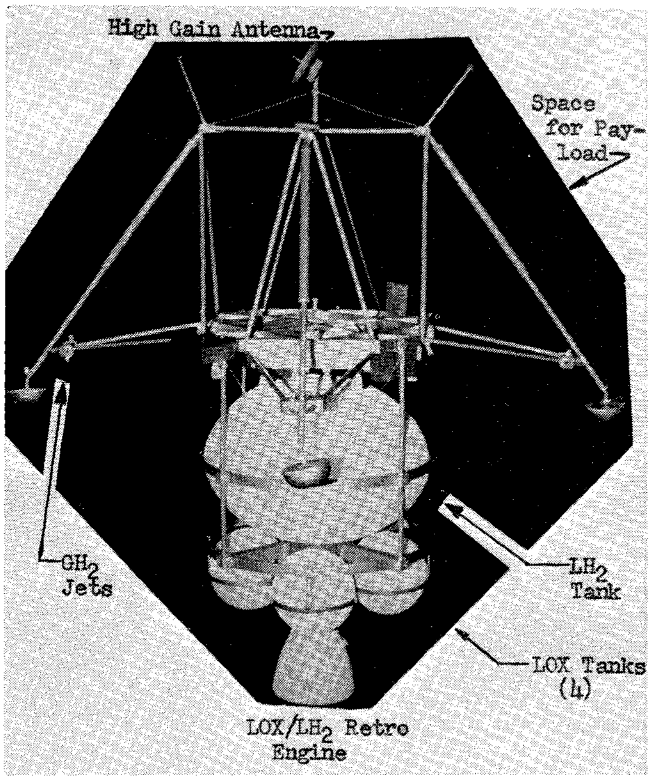

Fig. 1 Model of the lunar logistics vehicle.

It is anticipated that many LLV missions would be in support of manned explorations, and that the payload would consist of equipment that the astronauts will need on the lunar surface but cannot carry with them. Such payload may include a lunar flying unit, science payloads of various types e.g., "Apollo Lunar Science Experiment" (weighing up to 500 lb), a lunar expandable shelter (weighing about 1500 lb), various tools and supplies needed by the astronauts for an extended stay time on the moon, and, if required, a larger lunar roving vehicle. Missions not supporting man would carry experimental packages and, perhaps, devices for lunar mobility of the experiments.

The spacecraft is to soft-land at any selected site on the visible lunar face of the moon with a 3-sigma landing dispersion of one km. Cislunar flight times from 60 to 120 hr are contemplated.

Figure 1 shows the structure and the equipment which weighs approximately 9000 lbs when fully loaded with propellants, fuel cell reactants, and helium gas. The dimension of the spacecraft in the stowed condition is 150 in. in diam. × 210-in. long.

The lower part of the spacecraft forms the main retro propulsion unit and consists of a large liquid hydrogen tank (254 ft^3), four liquid oxygen tanks (each 18 ft^3), and the Pratt and Whitney RL 10A-3-3 engine developing a thrust of 15,000 lbf. This part of the structure is jettisoned after the main retro burns out. The empty main retro equipment and its supporting structure has an approximate mass of about 1000 lb; the tanks contain 5000 lb of LOX and 1000 lbs of LH_2.

Immediately above the LH_2 tank is the main lander structural platform. Mounted on the top of the platform is the payload and below the platform most of the lander subsystems.

Presented as Paper 70-613 at the AIAA 6th Propulsion Joint Specialist Conference, San Diego, Calif., June 15–19, 1970; submitted September 21, 1970; revision received October 9, 1970. Preliminary design of the vehicle[2,3] was performed by F. O. Calvert, J. H. Cole, F. M. Davidson, I. Eisenstein, C. M. Epps, G. E. Gless, G. F. Hauck, F. J. Hendel, B. Koo, S. J. Kozak, T. M. Perkins, A. J. Perna, G. Pincus, C. G. Richards, J. E. Robertshaw, J. E. Rozenberg, F. R. Swenson and J. M. Wampler under direction of S. L. Dickerson, C. J. Huang, D. B. Mackay, and A. N. Paul, all working under NASA Grant NSR 44-005-059 (1969 NASA-ASEE Institute in Houston, Texas). Support of R. Abel, B. Redd, R. Bristow, N. Chaffee, B. D. Kendrick, M. Lauston, P. G. Thomas, C. Vaughen, and others of NASA-MSC is gratefully acknowledged.

* Associate Professor, Aeronautical Engineering. Associate Fellow AIAA.